

THERMAL TRANSFORMATIONS OF RED WALL TILE PASTES

S. J. G. Sousa and J. N. F. Holanda*

Group of Ceramic Materials, Laboratory of Advanced Materials, State University of Northern Fluminense, 28013-602 Campos dos Goytacazes-RJ, Brazil

This work focuses on the thermal and mineralogical transformations of red wall tile pastes. The pastes contain different amounts of calcareous and are prepared with Brazilian raw materials. Thermal transformations are evaluated by TG, DTG and DTA, dilatometric analysis, and X-ray diffraction. Four endothermic transformations were identified and interpreted as the release of physically adsorbed water, dehydration of hydroxides, dehydroxylation of kaolinite, and decomposition of carbonate. An exothermic transformation within the 925–950°C range is associated to crystallization of new phases such as calcium aluminosilicates and mullite. TG measurements indicate that the total mass loss of the pastes is dependent on the amount of calcareous addition. Dilatometric analysis indicates the onset of sintering at around 900°C, leading to shrinkage of the pellets. The thermal analysis results agree well with the X-ray diffraction.

Keywords: red wall tiles, thermal analysis, X-ray diffraction

Introduction

Wall tile is a clay-based product employed in the interior of buildings. These products exhibits high porosity [1], particularly the open porosity. The NBR 13818 Brazilian standard [2] prescribes a value of water absorption above 10% (class BIII), which provides good adherence and less mass per square meter. The main raw materials used in the manufacture of wall tiles are kaolinic and illitic clays, and variable amounts of carbonate and quartz [3]. Each component of the paste contributes differently to the final properties of the product. Each raw material has a complex mineralogical composition. This makes the study of its thermal transformations rather difficult.

During sintering, the wall tile pastes undergo a series of physical and chemical transformations, which are characterized by thermal reactions and mass transfer processes. These transformations have different origins and take place at different temperature ranges. The knowledge about these transformations makes easier the control of the properties of the material.

There are important kaolinic sedimentary clay and calcareous deposits in South-Eastern Brazil [4]. These raw materials have not been used in the manufacturing of wall tile yet, although Brazil be the fourth worldwide producer of ceramic floor and wall tiles [5]. The reason for this situation is the lack of information about the reactions that take place between kaolinic clay, calcareous and fine-grained quartz during sintering.

This study focuses on the thermal transformations taking place during the sintering of three red wall tile pastes prepared with Brazilian raw materials. A wide range of techniques are used to evaluate these transformations: differential thermal analysis (DTA), thermogravimetry (TG), derivative thermogravimetric analysis (DTG), dilatometric analysis, and X-ray diffraction (XRD). The combination of them correlates the thermal reactions to the mineralogical changes of the red wall tile materials.

Experimental

Materials

Three red ceramic pastes typically used for manufacturing of porous wall tiles were formulated [6]. Their compositions are shown in Table 1. Kaolinic clay, calcareous and quartz from South-Eastern Brazil were used as starting materials. The chemical compositions of the raw materials, determined by X-ray fluorescence, are given in Table 2. The ceramic pastes are prepared by the dry process, using an intensive mixer. Information about the particle size of the pastes is given in Table 3.

Table 1 Ceramic wall tile pastes compositions (mass%)

| Pastes | Clay | Calcareous | Quartz |
|--------|------|------------|--------|
| M1 | 70 | 12 | 18 |
| M2 | 70 | 15 | 15 |
| M3 | 70 | 18 | 12 |

* Author for correspondence: holanda@uenf.br

Table 2 Chemical compositions (mass%) of the starting materials

| Material | SiO ₂ | Al ₂ O ₃ | Fe ₂ O ₃ | Na ₂ O | K ₂ O | CaO | MgO | MnO | TiO ₂ | P ₂ O ₅ | LoI* |
|------------|------------------|--------------------------------|--------------------------------|-------------------|------------------|-------|------|------|------------------|-------------------------------|-------|
| Clay | 46.42 | 27.90 | 9.10 | 0.36 | 1.67 | 0.22 | 0.71 | 0.11 | 1.32 | 0.21 | 11.96 |
| Calcareous | 6.01 | 0.81 | 0.55 | 0.15 | 0.23 | 47.26 | 4.91 | 0.01 | 0.06 | 0.07 | 39.94 |
| Quartz | 99.66 | 0.15 | 0.04 | — | — | — | — | — | 0.01 | — | 0.25 |

*LoI = loss on ignition

Table 3 Particle size data of the ceramic wall tile pastes

| Pastes | Fraction/% | | |
|--------|------------|-----------|--------|
| | <2 µm | 2≤x<60 µm | >60 µm |
| M1 | 31 | 63 | 6 |
| M2 | 30 | 65 | 5 |
| M3 | 32 | 62 | 6 |

Table 4 Measuring parameters of the STA data

| Parameter | Conditions |
|--|--|
| Temperature range | Ambient to 1150°C |
| Reference sample (Al ₂ O ₃) | Aluminum oxide (Al ₂ O ₃) |
| Sample pans | Pt |
| Balance sensitivity | 0.1 µg |
| ΔT sensitivity (DTA) | 0.001°C |
| Purge gas rate 'air' | 10 mL min ⁻¹ (TG) |
| Temperature calibration | Points three, Ag, Ir and Zn standards |
| Heating rate | 10°C min ⁻¹ |
| Sample mass/mg | |
| M1 | 24.47 |
| M2 | 24.70 |
| M3 | 24.36 |

Methods

X-ray diffraction analyses were performed with a Seifert URD-65 diffractometer, using monochromatic CuK_α radiation at 40 kV and 40 mA. The scanning speed was 1.5° (2θ) min⁻¹. The crystalline phases were identified from peak positions and intensity using reference data from the JCPDS files.

TG/DTG/DTA were carried out with a TA Instruments SDT-2960 simultaneous TG-DTA. The measuring parameters are summarized in Table 4. Dilatometric analysis of the samples were carried out on green wall tile pellets with a BP Engenharia RB-3000 dilatometer within the 25–1000°C range using a heating rate of 5°C min⁻¹ under air atmosphere.

Red wall tile pellets prepared by uniaxial pressing were sintered at 1110°C using a fast-sintering cycle of 60 min total time, including cooling. Mineral-

ogical analysis of the sintered pellets was carried out by X-ray diffraction. Microstructural analysis was done by scanning electron microscopy using a Zeiss DSM 962 SEM at 10 kV after gold coating.

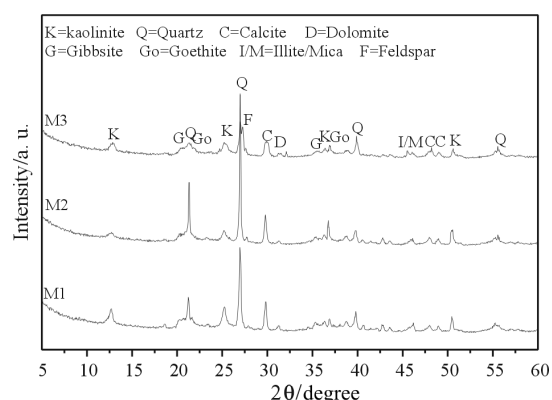
Results and discussion

Structural characterization

X-ray diffractograms of the red wall tile pastes are shown in Fig. 1. The following mineralogical phases were identified: kaolinite ($\text{Al}_2\text{O}_3 \cdot 2\text{SiO}_2 \cdot \text{H}_2\text{O}$), gibbsite ($\text{Al}_2(\text{OH})_6$), quartz (SiO_2), and calcite (CaCO_3). In addition, there are small amounts of illite/mica, goethite and feldspar. The X-ray diffraction data suggest that Al₂O₃ (Table 2) does not occur in its free form. Instead, it is bonded to the clay minerals and gibbsite structures. The chemical analysis of the clay powder (Table 2) also shows a moderate iron oxide content, expressed as Fe₂O₃. This oxide gives the reddish color of the wall tile pastes. The presence of goethite, as shown in Fig. 1, suggests that part of iron occurs in form of hydroxide. In addition, Fe³⁺ cations can partially substitute the Al³⁺ cations in the octahedral sites of the kaolinite structure [7, 8].

Thermal characterization

The analysis of the thermal behaviour of wall tile pastes is usually a difficult task due to its complex ceramic compositions [9]. The phase transformations play a significant role in the development of the

**Fig. 1** X-ray diffractograms of red wall tile pastes

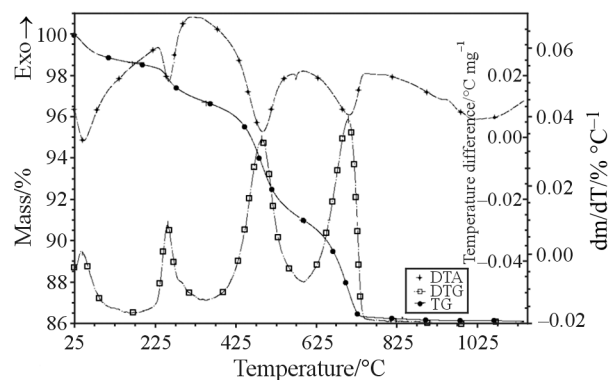


Fig. 2 TG/DTG/DTA curves of the red wall tile paste (sample M1)

microstructure of wall tiles. Therefore, they influence some porosity-related properties. The TG/DTG/DTA curves of the red wall tile samples are shown in Fig. 2. It is noticed that the samples behave very similarly, independently of their compositions.

Four endothermic events are seen in the DTA curves within the 42–44, 255–266, 489–495, and 704–719°C temperatures ranges, respectively. The first endothermic event concerns to the evolution of the physically adsorbed water by the kaolinite platelets [4]. The second endothermic event occurs due to the evolution of water vapor, resulting from the dehydration of hydroxides such as gibbsite and goethite. This is consistent with the results of X-ray diffraction. The third endothermic event within the 489–495°C temperature range is again caused by water evolution, but this time due to the dehydroxylation of kaolinite, which transforms into metakaolinite. The loss of the OH groups of the octahedral layer (the gibbsite layer)

distorts the atomic order of this layer, but the tetrahedra layer (silica layer) is less affected. The SiO_4 tetrahedra hold their form and a limited order is supposed to exist in the [110] plane [10, 11]. The fourth endothermic event within the 704–719°C range is related to the calcareous decomposition to form mainly calcium oxide and CO_2 degassing. However, X-ray diffraction (Fig. 1) showed also the presence of dolomite (MgCO_3). In fact the calcareous used is rich in calcite (CaCO_3), with dolomite and quartz as the major impurities [6]. Thus, decomposition reactions appear to occur simultaneously, resulting in CaO and MgO with predominance of CaO .

It was verified that the endothermic events are accompanied by an intense process of mass transfer in the samples as shown in the TG/DTG curves (Fig. 2) and summarized in Table 5. The samples presented a total mass loss during heating within the 13.72 to 16.96% range. The more is the amount of calcareous, the greater the mass loss is observed.

A large exothermic peak around 325°C due to the decomposition of organic matter is observed for all samples. It should be observed, however, that the organic matter is due mainly to the kaolinic sedimentary clay used as starting material [12].

An exothermic peak within the 925–950°C range observed for all samples is caused by further disruption of the silicate lattice to form new crystalline phases from metakaolinite. It seems that a series of thermal reactions, probably associated to the metakaolinite structural reorganization, could exist simultaneously and progressively in this temperature range. Pure kaolinite presents an exothermic peak at about 980°C, at which phases such as a Si-containing $\gamma\text{-Al}_2\text{O}_3$, a spinel structure or primary mullite can be

Table 5 TG/DTG and DTA results of the wall tile pastes

| Pastes | Mass loss TG/% | DTG _{max} / % °C ⁻¹ | DTA/°C | | | | | |
|--------|-------------------|--|-------------|-----|--------|------------|-----|--------|
| | | | Endothermic | | | Exothermic | | |
| | | | Onset | Max | Endset | Onset | Max | Endset |
| M1 | 1.34 | 43.7 | 25 | 44 | 175 | 875 | 925 | 1000 |
| | 1.90 | 256.1 | 175 | 256 | 375 | | | |
| | 5.71 | 489.7 | 375 | 490 | 625 | | | |
| | 4.77 | 704.5 | 625 | 704 | 825 | | | |
| M2 | 1.10 | 41.7 | 25 | 42 | 150 | 825 | 950 | 1000 |
| | 1.95 | 254.6 | 150 | 255 | 350 | | | |
| | 5.76 | 488.6 | 350 | 489 | 625 | | | |
| | 5.96 | 709.5 | 625 | 710 | 825 | | | |
| M3 | 1.56 | 42.7 | 25 | 43 | 195 | 800 | 950 | 1025 |
| | 2.23 | 266.2 | 195 | 266 | 400 | | | |
| | 5.73 | 494.8 | 400 | 495 | 625 | | | |
| | 7.44 | 718.9 | 625 | 719 | 800 | | | |

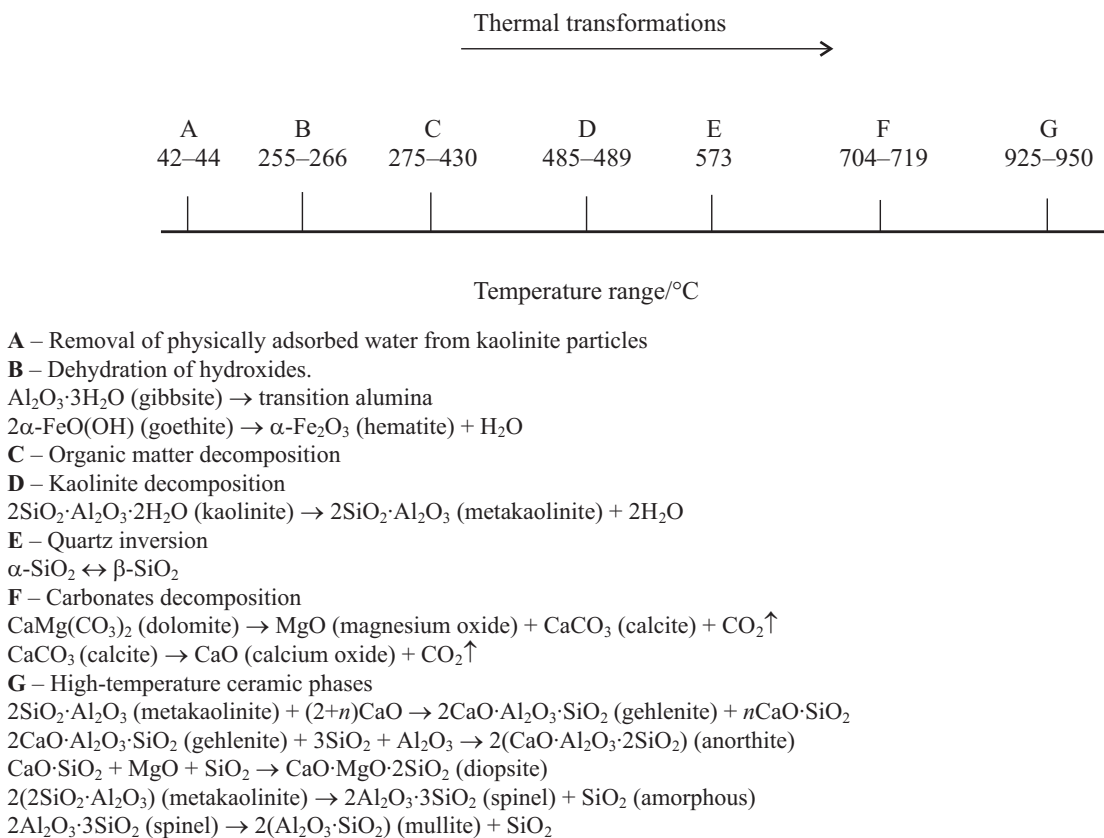


Fig. 3 Events occurring during heating of red wall tile pastes with corresponding reaction and temperature range

formed [13–15]. However, in the sintering process of carbonate bearing wall tile pastes, the preferential sequence of the reactions is given by [11, 16]: metakaolinite-gehlenite-anorthite. The metakaolinite is formed from kaolinite by removal of the hydroxyl groups of the silicate lattice at 489–495°C. Firstly, the gehlenite is formed as a metastable intermediate phase from metakaolinite and calcium oxide. The gehlenite structure is similar to a single layer structure of the metakaolinite. Thus, the occurrence of the same type of tetrahedra containing sheets suggests a topotactical transformation [11]. Later, anorthite is formed from gehlenite, which is combined with the silica and alumina rich phases due to the metakaolinite structure break, and the remaining fine quartz. In addition, the presence of impurities in the starting raw materials such as structural iron or iron oxide may influence the thermal transformations of metakaolinite-gehlenite-anorthite. Figure 3 outlines the thermal transformations occurring during sintering of the red wall tile paste at their respective temperatures and describes the possible reactions [4, 11, 13–17].

X-ray diffractograms of the pellets after sintering at 1110°C are presented in Fig. 4. X-ray diffraction indicated the presence of the following

phases: gehlenite ($2\text{CaO} \cdot \text{Al}_2\text{O}_3 \cdot \text{SiO}_2$), anorthite ($\text{CaO} \cdot \text{Al}_2\text{O}_3 \cdot 2\text{SiO}_2$), quartz (SiO_2), hematite (Fe_2O_3), and primary mullite. It can be observed also that the characteristic peaks (Fig. 1) of kaolinite, gibbsite, calcite, dolomite, and goethite present in the XRD of the pastes have disappeared. The quartz peaks remain. The hematite appears due to the iron present in the starting wall tile powder (Table 2). The reactions involving the formation of calcium aluminosilicate phases are according to the ternary phase diagram $\text{SiO}_2\text{-Al}_2\text{O}_3\text{-CaO}$ [16]. The red wall tile pastes, when plotted in this diagram [6], are located inside the field delimited by quartz, anorthite and mullite, although the pellets contain gehlenite as shown in Fig. 4. This indicates that some reactions that occur during sintering of the red wall tile pastes are kinetically governed by processes that do not reach the thermodynamic equilibrium.

The dilatometric curves of the ceramic pastes are presented in Fig. 5. As it can be seen, these curves are quite similar. The slight differences should be attributed to dissimilar proportions of quartz and calcareous (Table 1). Red wall tile pellets present an expansion until a peak at 500°C, followed by a small inflection between 500–600°C, probably due to $\alpha\text{-}\beta$ quartz transformation. This swelling is caused by the

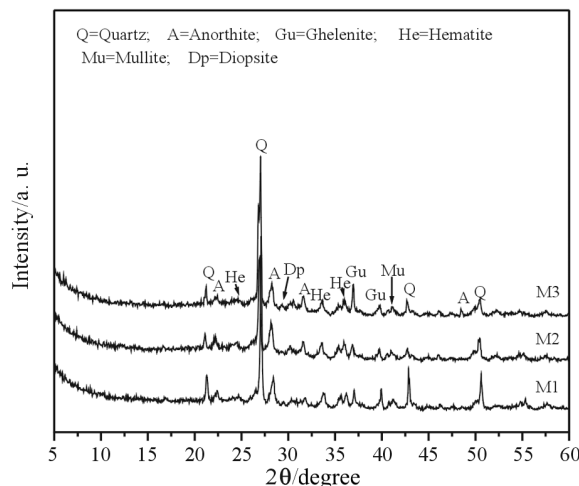


Fig. 4 X-ray diffractograms of red wall tile pastes sintered at 1110°C

thermal expansion of the starting materials, and has a maximum value of 2.5% for paste M3. In addition, the samples with higher content of calcareous presented a higher total swelling. After swelling, shrinkage is observed at about 600°C, probably due to the dehydroxylation of kaolinite that transforms into metakaolinite, as indicated by TG/DTG and DTA curves (Fig. 2). At about 650–750°C, a new swelling is observed, caused mainly by the CaCO_3 decomposition into CaO and CO_2 that evolves from the structure and contributes to the formation of its porosity. The CaO reacts then with metakaolinite, resulting in the formation of crystalline phases such as gehlenite and anorthite. These calcium rich crystalline phases have lower densities and therefore cause expansion of the structure. This expansion is responsible for important properties of the wall tile pellets such as high dimensional stability and high porosity. Figure 6 shows the typical microstructure of the red wall tile pastes

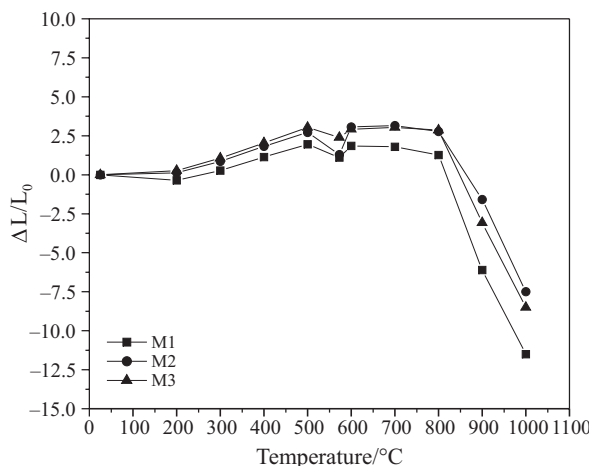


Fig. 5 Compiled dilatometric curves of the red wall tile pastes

sintered at 1110°C. High porosity connected with dense zones, resulting from carbonates decomposition are observed. The last step observed is a sharp shrinkage of the samples above 900°C. As it can be observed in the TG curves (Fig. 2), the wall tile pellets do not present mass loss above 900°C, indicating that decomposition reactions do not occur. Then, the shrinkage is probably caused by the onset of sintering, characterized by growth of the interparticle neck. In addition, the interparticle bonding in the pellets occurs with little formation of liquid phase, indicating that the sintering process is dominated by solid state sintering mechanisms. Without the surface tension forces exerted by a glassy viscous phase, the pellets shows little shrinkage on sintering and the bonding forces contributing to the mechanical strength of the pellets come from the new crystallized phases. It can be observed also that the increase of the calcareous amount (12 to 18 mass%) retards the sintering process of the pellets. These results confirm the complex thermal transformations of the wall tile pastes, and are consistent with X-ray diffraction and TG/DTG/DTA results.

The linear thermal expansion coefficient of the red wall tile pastes, $\delta = (\Delta L/L)/\Delta T$, is shown in Table 6. The value of δ depends on the phases (crystalline, glassy or amorphous), porosity, and the temperature range of interest. The results showed for all temperature ranges that the value of δ tends to increase due to the higher calcareous amount in the ceramic pastes.

Table 6 Coefficient of linear thermal expansion for the wall tile pastes

| Pastes | $\delta \cdot 10^{-7}/^\circ\text{C}^{-1}$ | | |
|--------|--|---------------------------------|---------------------------------|
| | $\delta_{25-300^\circ\text{C}}$ | $\delta_{25-600^\circ\text{C}}$ | $\delta_{25-800^\circ\text{C}}$ |
| M1 | 10.0 | 32.2 | 16.3 |
| M2 | 30.8 | 53.2 | 36.0 |
| M3 | 38.5 | 50.8 | 37.0 |

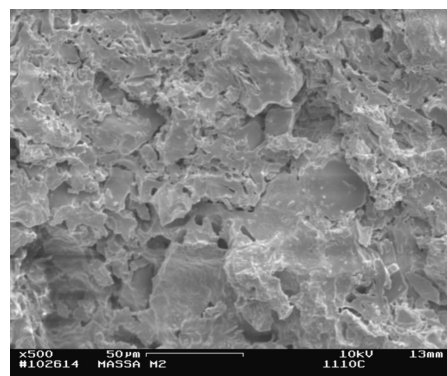


Fig. 6 SEM micrograph of red wall tile pastes (sample M2) sintered at 1110°C

The calcium carbonate rich calcareous increases the coefficient of thermal expansion due to the formation of Ca-based crystalline phases during sintering [18]. In addition, the higher value of $\delta_{25-600^\circ\text{C}}$ observed is related to the α - β quartz inversion.

Conclusions

The following conclusions may be drawn from the experimental results and their discussion.

DTA curves have shown that the red wall tile pastes undergo a complex series of endothermic and exothermic transformations involving: dehydration of hydroxides, decomposition of organic matter, dehydroxylation of clay mineral, carbonate decomposition, and phase transformations to form gehlenite, anorthite and mullite. It was also observed that the higher the calcareous amount the higher the mass loss, as supported by the endothermic events associated mainly to carbonate decomposition.

X-ray diffraction analysis of the pellets confirmed the mineralogical changes during sintering, which corroborate the TG/DTG/DTA results. However, it is probable that the sintering process does not reach equilibrium, resulting in incomplete reactions.

Dilatometric curves showed very clearly in which temperature ranges the pellets underwent expansion-shrinkage behaviour. It was also found that the shrinkage process around 900°C corresponds to the initial sintering of the pellets, likely by solid state sintering mechanisms.

Acknowledgements

The authors acknowledge the CNPq and CAPES for financial support, and to the Dr. R. Sánchez by the support in TG/DTG/DTA analysis.

References

- 1 A. Escardino, Tile & Brick Int., 9 (1993) 14.
- 2 ABNT – NBR 13818, Placas Cerâmicas Para Revestimento: Especificações e Métodos de Ensaio, Rio de Janeiro, Brazil, 1997, p. 78.
- 3 C. Fiori, B. Falbri, G. Donati and I. Venturi, *Appl. Clay Sci.*, 4 (1989) 461.
- 4 G. P. Souza, R. Sánchez and J. N. F. Holanda, *J. Therm. Anal. Cal.*, 73 (2003) 293.
- 5 G. Sezzi, *Ceram. World Rev.*, 48 (2002).
- 6 S. J. G. Sousa, Master Thesis, UENF-PPGECM, Campos-RJ, Brazil 2003.
- 7 R. S. T. Manhães, L. T. Auler, M. S. Strel, J. Alexandre, M. S. O. Massunaga, J. G. Carrió, D. R. Santos, E. C. Silva, A. Garcia-Quiroz and H. Vargas, *App. Clay Sci.*, 21 (2002) 303.
- 8 Y. Hu and X. Liu, *Miner. Eng.*, 16 (2003) 1279.
- 9 H. El-Didamany, H. H. Assal, H. S. Hassan and N. G. A. El-Ghafoor, *Ind. Ceram.*, 18 (1998) 91.
- 10 A. Gualtieri and M. Belloto, *Phys. Chem. Miner.*, 21 (1994) 442.
- 11 K. Traoré, T. S. Kabré and P. Blanchart, *Ceram. Int.*, 29 (2003) 377.
- 12 J. Alexandre, Ph.D Thesis, UENF-PPGCE, Campos-RJ, Brazil 2001.
- 13 P. S. Santos, Ciência e Tecnologia de Argilas. Vol. 1, 2nd Edn., Edgard Blücher Ltd., São Paulo 1989, pp. 282–288.
- 14 C. Y. Chen, G. S. Lan and W. H. Tuan, *Ceram. Int.*, 26 (2000) 716.
- 15 F. R. Alburquerque, B. Parent, S. J. G. Lima, C. A. Paskocimas, E. Longo, A. G. Souza, I. M. G. Santos and V. J. Fernandes Jr., *J. Therm. Anal. Cal.*, 75 (2004) 617.
- 16 M. M. Jórdan, T. Sanfelin and C. De la Fuente, *Appl. Clay Sci.*, 20 (2001) 87.
- 17 A. K. Chakraborty, *Thermochim. Acta*, 398 (2003) 203.
- 18 A. Barba, V. Beltrán, C. Felíu, J. García, F. Ginés, E. Sánchez and V. Sanz, Materias Primas Para la Fabricación de Soportes de Baldosas Cerámicas, 2^a Edición, Instituto de Tecnología Cerámica, Castellón, España 2002, pp. 268–271.

Received: March 20, 2006

Accepted: November 7, 2006

DOI: 10.1007/s10973-006-7030-7